Why does depth migration work so well in the plains?

2005 CSEG National Convention

Rob Vestrum, Thrust Belt Imaging; Brian Link, Kelman Technologies; John Mathewson, WesternGeco

Summary

If most of our fundamental imaging equations were originally designed for the case of horizontal strata, then why do we see significant imaging improvements when we apply depth migration in plains environments? Recent anisotropic depth migration projects from a variety of companies working in plains environments show significant improvements in seismic imaging. Examples range across a variety of stratigraphic settings and four independent imaging teams. We explore here some of the reasons why depth migration offers improved seismic imaging in a geologic setting that should honour the assumptions inherent in time processing. Although they are assumed negligible during the development of time-imaging equations, traveltime errors caused by the presence of rough topography, seismic anisotropy, and vertical velocity heterogeneity beyond the higher-order compensation for these effects will combine to reduce the accuracy of the seismic image. Reduced imaging accuracy may manifest itself in scattered amplitude distribution and/or decreased horizontal or temporal resolution.

Introduction

If we can more accurately describe traveltime effects that we see on offsets and migration operators, we can use higher fold on our image gathers, improving the signal-to-noise ratio and the integrity of the amplitudes. By raytracing through our velocity model, we get the most accurate description of the traveltimes that affect our seismic reflections, producing an improved seismic image. Our goal is to quantify the differences in traveltime calculations between the assumptions we make in time processing and the more computationally and interpretationally intensive depth processing.

The key difference between time imaging and depth imaging is in how we calculate the traveltime corrections used in the processing of seismic data. When we use analytic functions to describe traveltime effects in moveout and migration, we typically refer to these processes as time imaging. When we trace rays through a velocity model to calculate traveltime effects or we apply some other depth-consistent process like downward continuation, we are imaging in depth.

The fundamental equation for time imaging is the NMO equation, which describes the moveout curvature with respect to offset for a horizontal reflector follows:

$$t(x) = \sqrt{t_0^2 + \frac{x^2}{v^2}}, \qquad (1)$$

where $t(x)$ is the moveout time as a function of source-receiver offset, x, two-way zero-offset time, t_0, and the moveout velocity, v.

Some variations on the NMO equation correct for seismic anisotropy and vertical velocity heterogeneity, for example, Alkhalifah and Larner (1995) give an this expression for nonhyperbolic moveout that has a higher-order term than Equation 1. Their formulation corrects for VTI anisotropic traveltime effects and for the reduced traveltime with offset that occurs in the presence of vertical velocity gradients. Alkhalifah noted in a later paper (Alkhalifah, 1997) that there is an inherent ambiguity between the reduced traveltime with respect to offset caused by vertical velocity gradients and caused by the presence of VTI anisotropy. Even though their formulation corrects for some higher-order velocity effects, it still assumes a perfectly flat recording surface, which is appropriate for seismic data from marine environments, but there are significant traveltime effects from acquisition on a rough topographic surface.

Rough Topography

The first time-imaging approximation we look at is imaging below rough topography. Most plains environments that have perfectly flat layer-cake geology in the subsurface also have a rough topographic surface as a result of water drainage or glaciation. There are two ways to approach the moveout equation in the presence of rough topography: (1) using a single-square-root (SSR) equation that assumes a raypath between source and receiver that is symmetric about the reflection point and (2) using a double-square-root (DSR) equation that calculates a different raypath length for the source and receiver sides of the raypath, which allows for source and receiver to have different elevations.

Figure 1 shows a schematic diagram of an extreme case of a rough-topography imaging problem. The extreme nature of this example helps to illustrate the contrast between the two time-processing approaches and the raytraced approach to seismic imaging. The offset between source and receiver in this case is 3 km and the depth to the reflector from the receiver location is 1500 m. The source location is 900 m above the receiver elevation and 2400 m above the reflector.

Figure 1a illustrates the case where one was time processing using an SSR moveout equation (Equation 1). In this implementation, the trace is shifted to an elevation halfway between the source and receiver elevation. This method is computationally the fastest because we only need to calculate one square root. We assume here that the raypath length is the same on both sides of the reflection point.

Figure 1b illustrates the DSR calculation for this model. The two different right-angle triangles are where the two square roots enter the equation. Imaging practitioners (e.g., Grech et al., 2004) justify the additional computational effort required to calculate two square roots by the additional accuracy in traveltime calculations when calculating separate traveltimes for source and receiver raypaths. Note here that we have 560 m of lateral-position error at this offset. Again, this is an extreme case we designed for illustrative purposes, but the rough topographic surface will cause reflection amplitudes to appear in different CMP locations than we assume in time processing.

The raypath length is slightly longer than the true raypath length because we have not moved this seismic amplitude laterally into its proper subsurface position. Even in this extreme case, the raypath-length error will result in a mere 0.4% error in the traveltime calculation. The danger here is in the lateral-position error that results from the time-processing assumption.

Following our investigation of the rough-topography problem in principle, we look at the quantities for more common plains topographies. Figure 2a shows the raypath-length error and Figure 2b shows the lateral-position error, both as a function of the height of the topographic relief or the change in elevation between source and receiver. The case modelled here is similar to the case in Figure 1, with a source-receiver offset at 3000 m and the minimum depth to the reflector of 1500 m, i.e., 1500 m is the depth to the reflector from the source or the receiver, whichever has the lowest elevation.

With respect to the raypath-length error, which is proportional to the traveltime error in the constant-velocity case, the graph in this figure (Figure 2a) shows that the DSR equation yields more accurate raypath lengths and therefore more accurate traveltimes for elevation differences less than 500 m. In the more realistic range of less than 200 m, the traveltime errors from the DSR equation are vanishingly small. The lateral-position error (Figure 2b), however, shows a fairly significant lateral shifting of seismic energy at the far offsets even for small elevation differences. For example, at 100 m of topographic relief, the lateral-position error would be 90 m. Since the zero-offset trace would not shift at all and the lateral-position error would continually increase to the farthest offset, we would expect

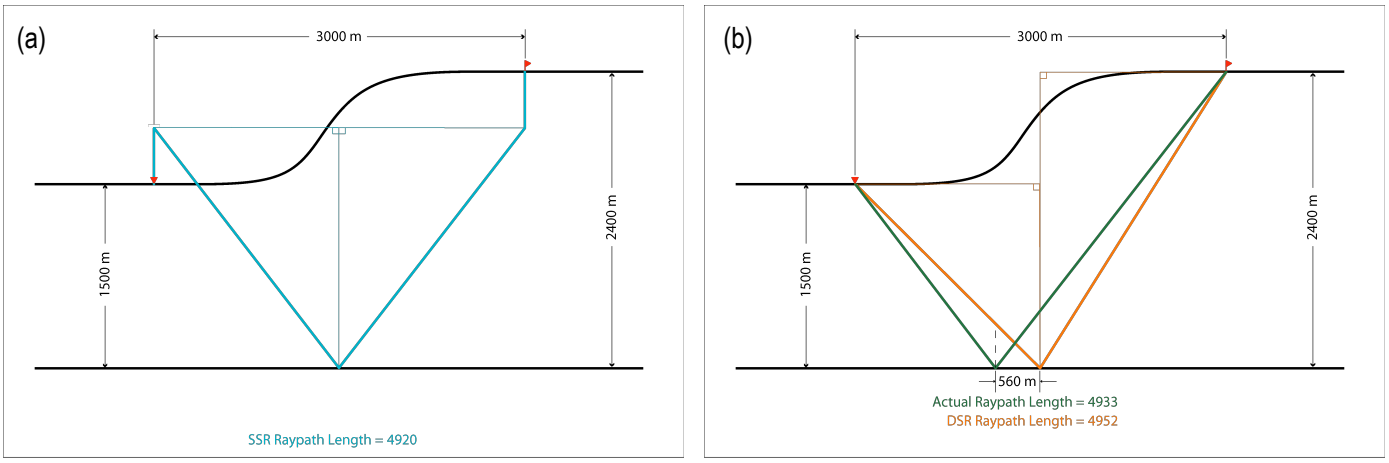

Figure 1: Ray pairs for the rough-topography case assuming isotropic, homogeneous velocities with a comparison of raypath lengths and assumed lateral position of the reflection amplitude. (a) Raypath calculated using single-square-root NMO and (b) raypath calculated using double-square-root NMO as compared to the actual reflection raypath.

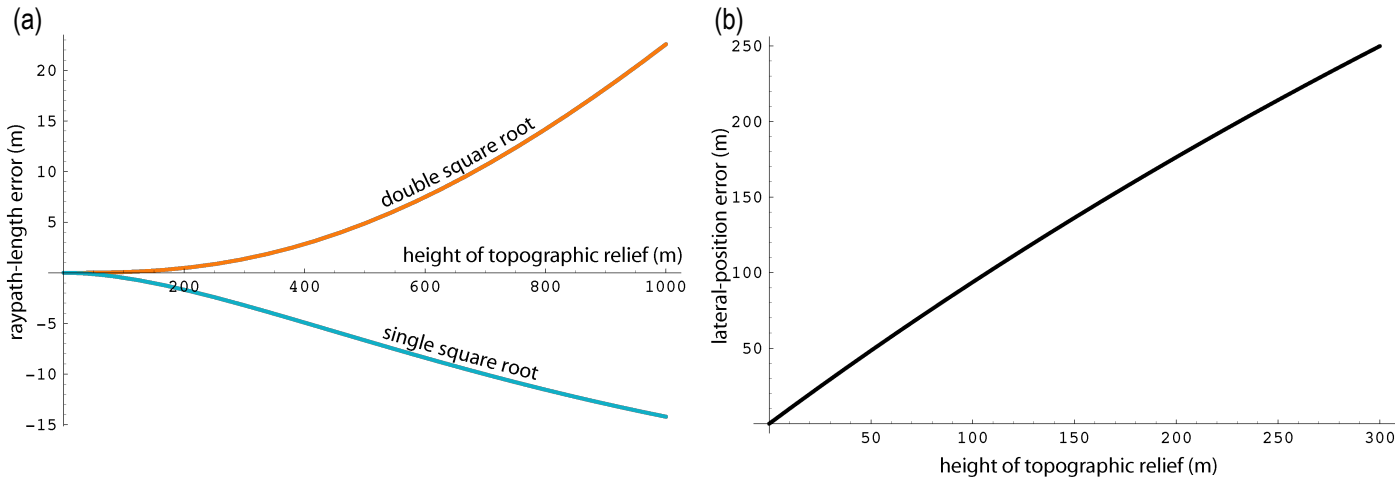

Figure 2: (a) Raypath-length error and (b) lateral-position error as a function of the height of the topographic relief between source and receiver locations.

to see a false AVO effect on the image gathers. No matter which time-processing methodology we use, we would expect to observe artificially lower amplitudes at the far offsets on the low side of this hill and higher amplitudes on the far offsets at the top of the hill.

Field data examples

Recently published examples from Veritas GeoServices (Holt et al., 2004) and Shell International (Peng and Steenson, 2001) show significant improvement in seismic imaging with the application of depth migration in a plains environment. Peng and Steenson (2001) had an exploration problem on a subtle stratigraphic play below laterally varying thickness of a layer above their target. They had a subtle lateral-velocity variation above their target, making this a classic, although subtle, depth-migration problem. Anisotropic depth migration improved their image and led to a successful well.

The velocity model in Holt et al. (2004) has minimal, if any, lateral-velocity variation, yet the improvements in seismic imaging are significant. The depth-migrated volume has sharpened edges of stratigraphic features and more continuous reflector continuity along horizons that are readily observable in the seismic displays in the abstract. More accurate traveltime corrections of velocity effects and imaging effects from the topographic surface led to superior illumination of subsurface reflectors and enabled a more aggressive drilling program.

Two yet-unpublished projects show similar improvements in seismic imaging in the plains. Depth imagers at Kelman Technologies recently completed a project in Western Canada. WesternGeco in Calgary has similar results from a 3D project in the state of New York, USA.

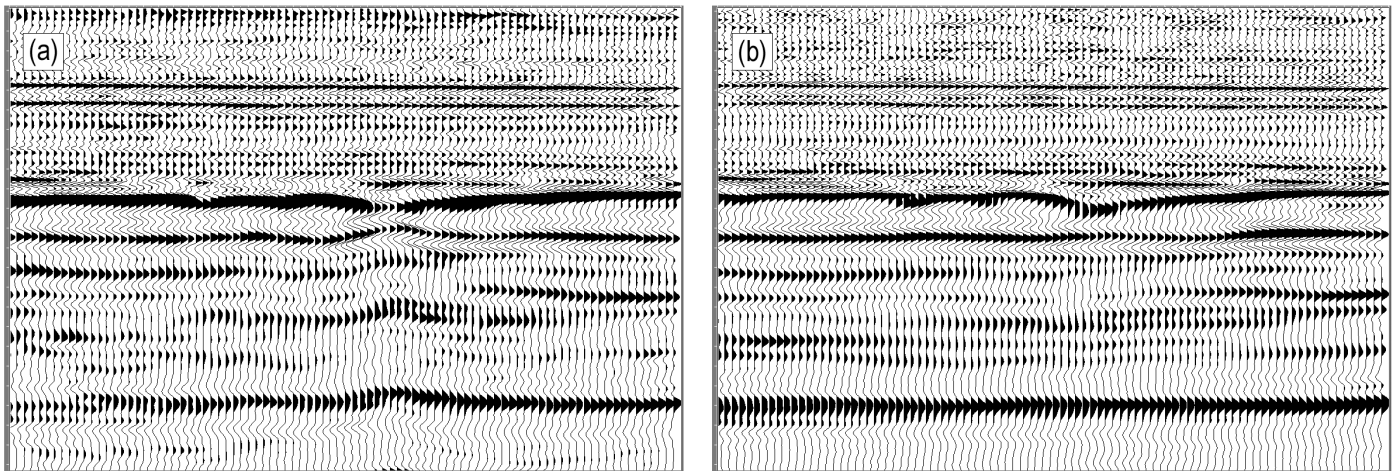

Figure 3: Comparison of inlines from (a) prestack time migration and (b) prestack anisotropic depth migration of a plains 3D seismic volume from Western Canada. Lines are displayed in depth.

At Kelman, the depth imaging work process forced the processing team to define a rigourous interval velocity model. Prestack velocity analysis showed a strong effective η. We backed out the vertical velocity heterogeneity effects from our effective η to reveal the anisotropic parameters, ε and δ. Eight horizons from ten wells went into the 3D tomographic inversion to finalize the velocity model. Figure 3 shows the final 3D anisotropic depth migration (Figure 3b) compared to the same inline slice from the time-migrated volume (Figure 3a). Note the increased lateral resolution of the edges of the collapsed structure and the improved amplitude continuity along the reflection events.

Depth imagers at WesternGeco have had a similar experience recently with another 3D anisotropic depth migration in the Eastern United States. Figure 4 shows the potential increase in lateral resolution on the seismic volume with the application of depth imaging. They accuracy of raytracing through an anisotropic velocity model derived from a tomographic inversion of reflection data brought out far more detail in the tectonic lineations that permeate these strata. Note also that the improved distribution of amplitudes on the depth-migrated volume (Figure 4b) minimized the acquisition-footprint lineations that run from the top to the bottom of the seismic slice in Figure 4a.

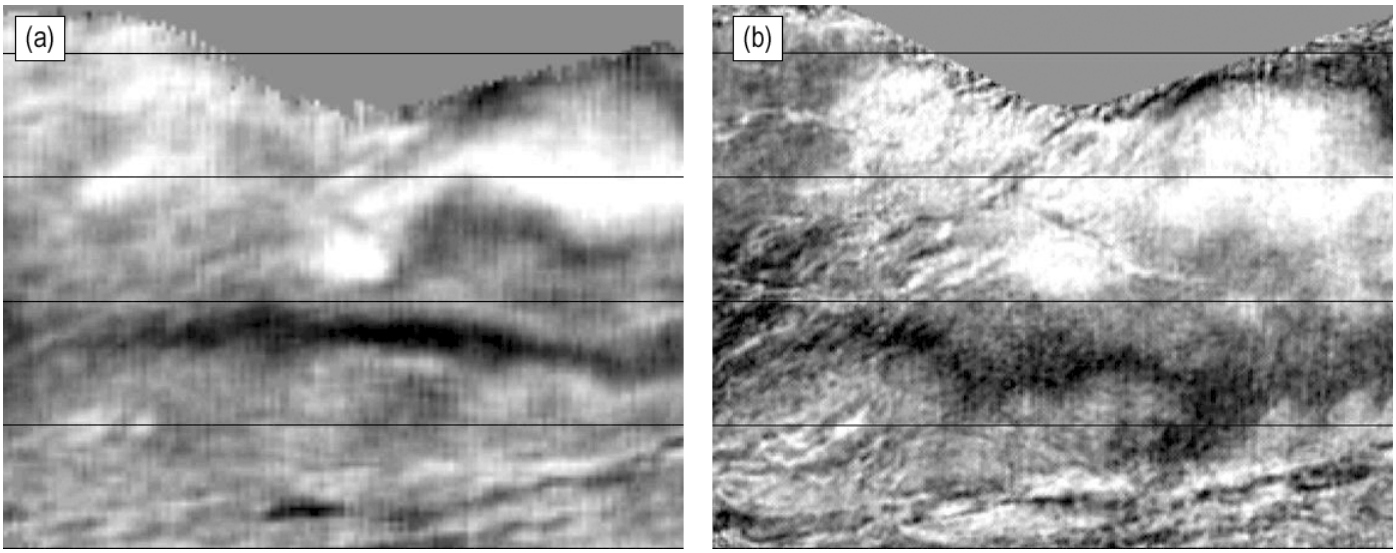

Figure 4: Comparison of lateral resolution on depth slices from (a) prestack time migration and (b) prestack anisotropic depth migration of a plains 3D seismic volume from Eastern US.

Conclusions

The increasing requirements for accuracy and resolution of seismic data are pushing the boundaries of time-processing assumptions. Even as time-processing algorithms improve to correct for higher-order velocity effects, small lateral variations in velocity and topography result in lateral shifting of energy that will affect AVO response of reflection amplitudes and reduce the lateral resolution of stratigraphic edges. Exploration examples from a variety of independent sources show the improvements in imaging accuracy in the presence of subtle velocity variation when depth imaging is applied to seismic data from plains environments. Improved amplitude distribution in the depth migration of the Eastern US dataset minimized lineations from the acquisition geometry that were readily apparent on the time-processed volume.

References

Alkhalifah, T. and Tsvankin, I., 1995, Velocity analysis for transversely isotropic media: Geophysics, Soc. of Expl. Geophys., **60**, 1550-1566.

Alkhalifah, T., 1997, Velocity analysis using nonhyperbolic moveout in transversely isotropic media: Geophysics, Soc. of Expl. Geophys., **62**, 1839-1854.

Holt, R., Joy, H., Culver B., and Cheadle, S., 2004, Optimum Stratigraphic Imaging with 3D Anisotropic Prestack Depth Migration: 2004 Natnl. Mtg., Can. Soc. Expl. Geophys.

Kirtland Grech, M.G., Cheadle, S., Miao, X., and Zhu, T., 2004, A velocity analysis procedure for multicomponent data with topographic variations: 2004 Natnl. Mtg., Can. Soc. Expl. Geophys.

Peng, C. and Steenson, K.E., 2001, 3-D prestack depth migration in anisotropic media: A case study at the Lodgepole reef play in North Dakota: The Leading Edge, **20**, no. 5, 524-527.